

## **SURFACE FINISH CONTROL IN MACHINING PROCESSES USING TEXTURAL DESCRIPTORS BASED ON MOMENTS**

**Barreiro, J.; Alaiz, R.; Alegre, E. & Ablanedo, D.**

### **Abstract:**

*This paper presents a method to perform a surface finish control using a computer vision system. The goal pursued was to design an acceptance criterion for the control strategy. Class 1 would contain those parts with low roughness—acceptable—and class 2 those with high roughness—defective.*

*We have used 140 images obtained from AISI 303 stainless steel machining.*

*Images were described using five different methods – Hu, Flusser, Taubin, Zernike and Legendre moments.*

*Classification was done using k-nn and neural networks. With k-nn the best error rate – 4.7% – was achieved using Hu and Flusser descriptors.*

*With the neural network, a ten node hidden layer network with 300 cycles using Legendre descriptors leads to the optimal configuration – 4.7% error rate.*

*Key words: roughness control, textural descriptors, moments descriptors, k-nn, neural network classification.*

### **1. INTRODUCTION**

Some properties play a significant role in the surface finish of machined parts. These properties are directly related to the surface finish grade, which is determined by the manufacturing processes and the materials used. Thus, measurement of the surface finish grade has been a matter of special interest in the machining research during the last fifty years. The surface finish can be estimated by means of some roughness parameters defined in international standards [1]. Development of these

standards is basically oriented to tactile measuring devices that provide two-dimensional records of part profile. Nevertheless, surface measurement technologies have significantly evolved during last decades, from the first analogical contact devices to the current digital techniques [2].

Among modern techniques, those based on computer vision can be remarked. The advantages this technology provides are diverse. Whereas tactile techniques characterize a linear track over the part surface, computer vision techniques allow characterizing wide areas of the part surface providing more information [3-5]. Also, computer vision techniques take measures faster, since images are captured in a very short time, and they can be in-machine implemented. In addition, the application of exhaustive validity checking to each part is also possible. This aspect would be very difficult to achieve with traditional tactile profilometers, which are slow and delicate.

Continuous advances have been made in sensor technologies. Particularly, vision sensors have been greatly enhanced in capabilities and price decrement. Additionally, advances in image processing technology provide more reliable conclusions than before.

In all, computer vision is a very interesting technology for industrial environment. The use of these systems for the monitoring of operations in machining has proved [6, 7] an important reduction in the cycle time and the required resources. As far as the traditional contact techniques are concerned, computer vision techniques use

other parameters to measure the surface finish. In the light of this perspective, the current standards developed for tactile devices do not reflect the current state of technology. New procedures are necessary to correlate the results obtained by tactile instruments with those obtained with other type of devices, as those based on computer vision. In this context, two lines should be remarked: the study on the spatial domain and the study in the frequency domain. This work tackles the measurement of surface quality from the point of view of the spatial domain.

Tarng and Lee [8] and Lee et al. [9] analyze the artificial vision and image analysis systems to quantify the roughness in different turning operations. Methods based on image analysis capture an image of the surface and analyze its pixels to obtain a diffuse light pattern. Later on, roughness parameters are calculated by means of statistical descriptors. One of the most used parameters is the standard deviation of gray levels. Kumar et al. [10] focus on milling, turning and molding processes. They make zoom over original images to obtain the  $G_a$  parameter (the image gray level average), finding a high correlation amongst the  $G_a$  parameter and the surface roughness. Al-Kindi ET al. [3] propose a method named intensity-topography compatibility (ITC), characterizing the image data by three components: lightning, reflectance and surface characteristics. They calculate the value of conventional roughness parameters combining statistical such as mean value and standard deviation. Lee et al. [6] developed a computer vision system that measures the roughness in turning processes automatically.

The rest of the paper is organized as follows: Sect. 2 describes the image acquisition process. Image procession is included in Sect 3 and the classification stage in Sect. 4. Finally, conclusions are summarized in Sect. 5.

## 2. SAMPLES AND IMAGE ACQUISITION

### 2.1 Test parts and machining characteristics

Test parts were made of AISI 303 X8CrNiS18-9 stainless steel. This material was chosen due to the wide use in the small part mass-manufacturing industry. A MUPEM CNC multi-turret parallel lathe —ICIAR/1/42 model— was used for the machining of parts.

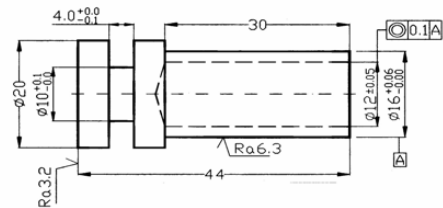


Fig. 1. Test part.

The test part is showed in **Fig. 1**. Several part operations were carried out, all of them representative of massive precision machining. However, only the cylindrical shape was used for surface finish measurement. Cutting tools were coated carbide inserts from Sandvik. The machining parameters used for the tests were fixed at the following values: cutting speed 250 m/min, feed rate 0.27 mm/rev and cutting depth 2 mm, considered as reference values. A surface finish control was performed on a HOMMEL-WELKE class 1 perfilometer. It was evident that the evolution of surface finish Ra values was far worse when increasing the machining time.

### 2.2 Image acquisition

Images of the parts were captured using a specific location fixture which had attached a camera and a diffuse lighting system (Figure 2). The part was positioned onto a 'V' shape bracket. The lighting system comprised a FOSTEC regulated light source DCR RIII. A NER SCDI-25-F0 diffuse illumination SCDI system was used to avoid shines. The system provided diffuse illumination in the camera axis.

The images were obtained using a Pulnix PE2015 B/W camera with 1/3" CCD. A Matrox Meteor II frame grabber card was used to digitize the images.

The optic assembly was composed of an OPTEM industrial zoom 70XL, with an extension tube of 1X and 0.5X/0,75X/1.5X/2.0X OPTEM lens. We used the maximum magnification of the system.



Fig. 2. Acquisition system.

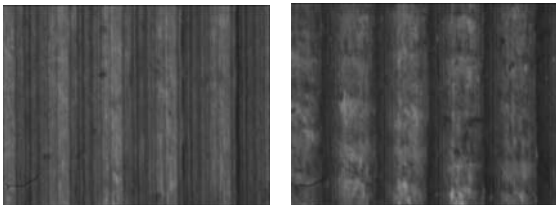


Fig. 3. Original images with Ra of 2.47 $\mu$ m -upper- and 4.33  $\mu$ m -lower.

### 2.3 Experimental sets of images

Using such system, 143 images were captured (see Fig. 3). Each of the images was labelled with its Ra roughness parameter, obtained using the median of three repeated Ra measuring. The roughness values were in the range 2.40 to 4.33  $\mu$ m. Several experiments were carried out and the images were divided in two sets: the first class corresponds to low roughness (satisfactory) and the second class to high roughness (unacceptable). Three different cases were considered. In the first case, the first thirty images (ordered by Ra values) were separated from the last thirty. In the second case, one class was composed by the first fifty images and the second one by the last fifty. In the third case, seventy of them were

assigned to class 1 while the other seventy to class 2.

## 3. IMAGE PROCESSING AND FEATURE EXTRACTION METHODS

### 3.1 Image pre-processing

A vertical Prewitt high pass filter was applied to the complete set of images in order to enhance contrast and make easier the description of roughness. Later on, five sets of descriptors were obtained for the original images and also for the filtered images. Fig. 3 shows images before filtering and Figure 4 shows the same images after filtering.

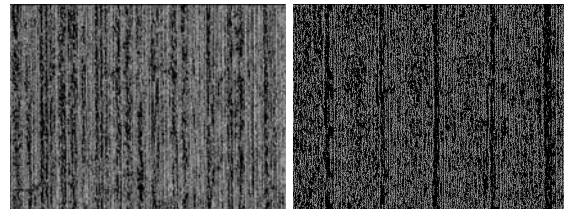


Figure 4. Filtered images with Ra of 2.47  $\mu$ m -upper- and 4.33  $\mu$ m -lower.

### 3.1 Texture descriptors

Five different feature vectors were obtained by computing some texture descriptors based on moments: seven moments of Hu, six moments of Flusser, eight moments of Taubin, the moments of Zernike up to order 6 (16 features) and Legendre moments up to order 2 (9 features).

## 4. CLASSIFICATION METHODS

The former feature vectors were classified by means of k-nn using the 'random sampling' validation method. This let us to compare the results of classification with those obtained by means of neural networks. The neural network used was a multilayer Perceptron, with an output layer with two nodes for the classification into the low or acceptable roughness class and the high or unacceptable class. The number of nodes in the input layer was determined considering the dimension of input patterns in each case, which runs from six features

corresponding to the Flusser descriptors until sixteen features corresponding to Zernike descriptors. The optimum number of nodes in the hidden layer and training cycles have been selected empirically. The learning algorithm belongs to the group of ‘back propagation’ algorithms, in particular the Levenberg-Marquadt optimized version.

The method of validation is a ‘random sampling’ type. This method divided the available set of images in subgroups randomly, 70% for training and 30% for test. The iterative process was repeated ten times and the mean error was calculated.

Also, the effect of data normalization over the classification error was analyzed. The feature vector values were normalized, in such a way that a translation and a scaling were applied to each random sampling extracted from the training set. The translation of the group of vectors was applied from its own centroid to the origin of the space in order to achieve a medium value of zero. The scaling was done dividing each vector by the medium energy of the group, calculated as the root mean square. This operation leads to a standard deviation value of one.

#### 4.1 k- nearest neighbours

The best results have been achieved with the orthogonal moments of Zernike and Legendre and also with the invariants moments of Hu. The lower error is 5% approximately for the cases of thirty and fifty images by class and the low class has a superior rate of failure. The error increases up to 10% when using seventy images and the error distribution is fairly uniform among the classes. Table 1 shows the minimum errors in each class for the three descriptors that show the best results.

Hu		Zernike		Legendre		# Ima
Low	High	Low	High	Low	High	
10.33	3.33	7.78	2.22	8.89	4.44	30
8.00	4.00	9.33	2.00	8.00	3.33	50
10.95	9.05	10.00	8.57	10.95	9.52	70

Table 1. Minimal errors in each class.

#### 4.2 Neural network

The error rates obtained with the neural network training are similar, lower than 10% for several descriptors. The error rate was 4.67% with fifty images in each class and using the Legendre descriptors. All descriptors enhance their results when using the vertical Prewitt filtering, with the exception of Zernike descriptors whose behaviour is just the opposite.

All descriptors were used for this test except Taubin descriptors. The reason is that the poor results obtained with Taubin descriptors indicate that they are not adequate for this problem.

	100	300	500	1000	1500
<b>Hu</b>					
<b>1</b>	13.89	29.44	13.89	18.89	20.00
<b>5</b>	26.67	17.22	17.78	20.00	14.44
<b>10</b>	20.56	13.33	17.78	17.22	20.56
<b>15</b>	24.44	22.22	20.56	15.56	21.11
<b>Zernike</b>					
<b>1</b>	40.56	47.22	43.33	42.22	47.78
<b>5</b>	46.67	50.00	44.44	45.56	40.56
<b>10</b>	44.44	43.89	35.00	40.00	40.00
<b>15</b>	36.67	38.33	41.67	39.44	41.67
<b>Legendre</b>					
<b>1</b>	16.67	16.11	20.56	17.22	24.44
<b>5</b>	11.67	16.67	15.00	16.11	23.89
<b>10</b>	13.89	16.67	26.67	13.33	20.56
<b>15</b>	15.56	10.00	9.44	13.89	10.00
<b>Flusser</b>					
<b>1</b>	23.33	27.78	23.89	37.22	26.11
<b>5</b>	29.44	31.11	35.00	34.44	32.78
<b>10</b>	32.22	30.56	32.78	32.22	22.78
<b>15</b>	35.56	33.89	27.78	27.78	36.11

Table 2. Error rates. Classes with 30 images filtered with Prewitt.

Table 2 shows the global error rate for the case of thirty images in each class and using only filtered images, since the best results are obtained with them. The values in the first row and first column are the number of cycles and the number of nodes in the hidden layer, respectively.

Table 3 and 4 shows the global error rate for the other cases, that is, fifty and seventy images in each class. It is observed that the lower error rates correspond to the fifty images case, even better than those obtained with thirty images.

The reason of this behaviour may be that, in the case of thirty images, the training set is not wide enough for optimum network learning and a reliable classification.

In the case of seventy images the error rates increase up as expected, since values near to the decision border in both classes are very close.

	100	300	500	1000	1500
<b>Hu</b>					
<b>1</b>	10.33	17.33	9.67	16.33	11.33
<b>5</b>	15.00	19.67	14.67	23.00	15.67
<b>10</b>	14.00	12.33	13.33	13.00	11.00
<b>15</b>	9.67	18.33	22.00	11.33	16.33
<b>Zernike</b>					
<b>1</b>	35.33	42.33	36.00	37.67	32.67
<b>5</b>	46.67	45.67	43.00	48.67	49.33
<b>10</b>	45.33	49.00	43.00	44.67	43.00
<b>15</b>	45.33	42.33	46.00	42.00	46.00
<b>Legendre</b>					
<b>1</b>	27.00	13.67	15.33	19.67	30.33
<b>5</b>	12.33	12.67	8.67	15.33	8.00
<b>10</b>	10.67	4.67	5.33	8.00	15.00
<b>15</b>	9.33	12.00	9.00	5.67	8.33
<b>Flusser</b>					
<b>1</b>	30.33	14.00	15.67	18.33	30.67
<b>5</b>	17.67	23.33	22.00	20.00	27.33
<b>10</b>	29.67	34.00	30.00	31.33	35.67
<b>15</b>	26.00	40.00	28.00	29.33	30.33

Table 3. Error rates. Classes with 50 images filtered with Prewitt

	100	300	500	1000	1500
<b>Hu</b>					
<b>1</b>	24.05	19.52	26.19	22.86	19.29
<b>5</b>	19.29	14.29	21.67	21.90	19.05
<b>10</b>	19.05	13.81	19.76	16.43	14.52
<b>15</b>	13.57	19.76	19.05	25.71	15.48
<b>Zernike</b>					
<b>1</b>	31.19	24.05	25.00	19.29	37.86
<b>5</b>	48.10	44.76	46.19	45.24	42.14
<b>10</b>	46.90	45.48	46.90	47.38	43.33
<b>15</b>	44.76	43.33	44.05	49.29	43.33
<b>Legendre</b>					
<b>1</b>	27.38	26.90	24.52	18.81	35.95
<b>5</b>	24.76	16.67	25.71	22.62	17.86
<b>10</b>	22.62	20.48	16.19	20.71	18.81
<b>15</b>	21.90	16.90	19.76	17.86	15.24
<b>Flusser</b>					
<b>1</b>	21.90	21.67	25.71	32.38	17.38
<b>5</b>	30.24	23.57	28.57	24.52	16.67
<b>10</b>	28.57	18.57	29.76	25.48	26.67
<b>15</b>	31.90	34.29	25.00	29.76	30.95

Table 4. Error rates. Classes with 70 images filtered with Prewitt.

### 4.3 Minimal errors

Table 5 and 6 show the minimal errors obtained with each descriptor and with both classification methods. The **n** parameter indicates that feature vectors are normalized. It can be observed that the KNN classifier gives better results in all cases.

# Images	Classification	Hu	Zernike
30	KNN	6.67	5
	KNN n.	10	17.78
	MLP	13.3	36.7
	MLP n.	-	-
50	KNN	5.67	5.67
	KNN n.	4.67	22.33
	MLP	9.7	32.7
	MLP n.	12.67	18.67
70	KNN	10	9.29
	KNN n.	7.86	20.24
	MLP	13.6	19.3
	MLP n.	15.95	18.33

Table 5. Minimal errors with Hu and Zernike descriptors.

#.	Class.	Legendre	Flusser	Taubin
30	KNN	6.67	19.44	42.22
	KNN n.	11.67	6.67	32.78
	MLP	9.4	22.8	-
	MLP n.	-	-	-
50	KNN	5.67	20.33	34.33
	KNN n.	22.67	4.67	36.33
	MLP	4.7	14	-
	MLP n.	5.33	11	-
70	KNN	10.24	31.9	45.19
	KNN n.	13.57	10.95	40.71
	MLP	15.2	16.7	-
	MLP n.	11.43	15.48	-

Table 6. Minimal errors with Legendre, Flusser and Taubin descriptors.

## 5. CONCLUSION

This paper proposes a method to carry out the quality of surface finish of machined metallic parts. The performance of five different sets of descriptors was analyzed, applied on both filtered and unfiltered images. In general, filtered images showed a better performance. The best results were achieved using k-nn classification, with normalized data and Flusser and Hu

descriptors, obtaining an error rate of 4.67%. Results achieved with a MLP neural network were similar in terms of the error rate.

The results show that the use of texture descriptors is a feasible method to evaluate the roughness of metallic parts in the context of product quality.

## 6. ACKNOWLEDGMENTS

This work has been partially supported by the research projects DPI2006-02550 supported by the Spanish Ministry of Education and Science, ULE2005-01 by the University of León and LE018B06 by the Junta de Castilla y León.

## 7. REFERENCES

1. ISO4288:1996. Geometrical product specification (GPS) – Surface texture: Profile method.
2. Al-Kindi, G.A. & Shirinzadeh, B. An evaluation of surface roughness parameters measurement using vision-based data. *Intl. J. of Mach. Tools & Manuf.*, 2007, **47**, 697-708.
3. Al-Kindi, G.A.; Baul, R. & Gill, K. An application of machine vision in the automated inspection of engineering surfaces. *Intl. J. of Production Research*, 1992, **30** (2), 241-253.
4. Senin, N.; Ziliotti, M. & Groppetti, R. Three-dimensional surface topography segmentation through clustering. *Wear*, 2007, **262**, 395-410.
5. Schmahling, J.; Hamprecht, F.A. & D.M.P. Hoffmann. A three-dimensional measure of surface roughness based on mathematical morphology. *Intl. J. of Machine Tools & Manufacture*, 2006, **46**, 1764-1769.
6. Lee, B.; Juan, H. & Yu, S. A study of computer vision for measuring surface roughness in the turning process. *Intl. J. of Advanced Manufacturing Technology*, 2002, **19**, 295-301.
7. Castejón, M.; Alegre, E.; Barreiro, J. & Hernández, L.K. On-line tool wear monitoring using geometric descriptors from digital images. *Intl. J. of Machine Tools & Manufacture*, 2007, **47**, 1847-1853.
8. Tarng, Y. & Lee, B. Surface roughness inspection by computer vision in turning operations. *Intl. J. of Machine Tools & Manufacture*, 2001, **41**, 1251-1263.
9. Lee, S. & Chen, C. On-line surface roughness recognition system using artificial neural networks system in turning operations. *The International Journal of Advanced Manufacturing Technology*, 2003, **22** (7-8), 498-509.
10. Kumar, R.; Kulashekar, P.; Dhana-sekar, B. & B. Ramamoorthy. Application of digital image magnification for surface roughness evaluation using machine vision. *Intl. J. of Machine Tools & Manufacture*, 2005, **45**, 228-234.

## 8. CORRESPONDING ADDRESS

PhD. Joaquín Barreiro  
Dept. of Mechanical, Informatics and  
Aerospatiale Engineering.  
University of León, 24071 León, Spain.  
Phone: +34 987 291792,  
Fax: +34 987 291930,  
E-mail: [joaquin.barreiro@unileon.es](mailto:joaquin.barreiro@unileon.es)